

Validation of near infrared spectroscopy as an age-prediction method for plastics

Original

Validation of near infrared spectroscopy as an age-prediction method for plastics / Alassali, Ayah; Picuno, Caterina; Bébien, Tom; Fiore, Silvia; Kuchta, Kerstin. - In: RESOURCES, CONSERVATION AND RECYCLING. - ISSN 0921-3449. - STAMPA. - 154:(2020), p. 104555. [10.1016/j.resconrec.2019.104555]

Availability:

This version is available at: 11583/2769512 since: 2019-11-25T15:12:31Z

Publisher:

Elsevier

Published

DOI:10.1016/j.resconrec.2019.104555

Terms of use:

This article is made available under terms and conditions as specified in the corresponding bibliographic description in the repository

Publisher copyright

Elsevier postprint/Author's Accepted Manuscript

© 2020. This manuscript version is made available under the CC-BY-NC-ND 4.0 license
<http://creativecommons.org/licenses/by-nc-nd/4.0/>. The final authenticated version is available online at:
<http://dx.doi.org/10.1016/j.resconrec.2019.104555>

(Article begins on next page)

Manuscript Number: RECYCL-D-19-01551R2

Title: Validation of near infrared spectroscopy as an age-prediction method for plastics

Article Type: Full Length Article

Corresponding Author: Professor Silvia Fiore, PhD

Corresponding Author's Institution: Politecnico di Torino

First Author: Ayah Alassali

Order of Authors: Ayah Alassali; Caterina Picuno; Tom Bebien; Silvia Fiore, PhD; Kerstin Kuchta

Abstract: This work has two aims. Firstly, to validate the ability of experimental models derived through near infrared spectroscopy for acrylonitrile butadiene styrene (ABS), low-density polyethylene (LDPE), polyethylene terephthalate (PET), and polypropylene (PP) in predicting polymers' aging; focusing on the degree of oxidation. Secondly, to assess the reliability of non-invasive age-predictive models on waste plastic samples and on mechanically recycled samples. Aging time, temperature and number of extrusion cycles were selected as independent variables to build the aging-prediction models, where they were calibrated on samples subjected to controlled conditions. The accuracy of the prediction models was assessed on external samples (aged under known conditions) through the cross correlation technique and the Root Mean Square Error (RMSE). The models exhibited good collinearity for the aging temperature and the number of extrusion cycles factors for all tested polymers, but not for the aging time factor. The RSME value of the aging time factor was far from zero for all polymers. Plastic waste samples provided analogous results; the aging time estimation was mostly negative in value. The estimations of aging time and number of extrusion cycles were always positive in values, where the most reasonable aging factor estimation was the number of extrusion cycles.

- We investigated NIR spectroscopy ability to predict the oxidation degree of polymers
- Aging-prediction models were experimentally derived for ABS, PE, PET and PP
- Aging time, temperature and no. of extrusion cycles were the independent variables
- The models were calibrated on artificially aged samples and waste polymers
- The no. of extrusion cycles proved to be a key parameter for the reliability of the models

1 **Validation of near infrared spectroscopy as an age-prediction method** 2 **for plastics**

3

4 Ayah Alassali ^a, Caterina Picuno ^a, Tom Bébien ^b, Silvia Fiore ^{c, *}, and Kerstin Kuchta ^a

5

6 ^a TUHH – Hamburg University of Technology, Institute of Environmental Technology and
7 Energy Economics, Waste Resources Management, Harburger Schlosstr. 36, 21079
8 Hamburg, Germany9 ^b National Institute of Applied Sciences of Lyon (INSA), 20 Avenue Albert Einstein,
10 69100 Villeurbanne, France11 ^c DIATI (Department of Engineering for Environment, Land and Infrastructures),
12 Politecnico di Torino, 24, corso Duca degli Abruzzi, 10129 Turin, Italy

13

14 ***Corresponding author:** prof Silvia Fiore, DIATI, Politecnico di Torino, Corso Duca
15 degli Abruzzi, 24; 10129, Torino, Italy; Email: silvia.fiore@polito.it; Phone: +39 011
16 0907613

17

18 **Abstract**

19 This work has two aims. Firstly, to validate the ability of experimental models derived
20 through near infrared spectroscopy for acrylonitrile butadiene styrene (ABS), low-density
21 polyethylene (LDPE), polyethylene terephthalate (PET), and polypropylene (PP) in
22 predicting polymers' aging; focusing on the degree of oxidation. Secondly, to assess the
23 reliability of non-invasive age-predictive models on waste plastic samples and on
24 mechanically recycled samples. Aging time, temperature and number of extrusion cycles
25 were selected as independent variables to build the aging-prediction models, where they
26 were calibrated on samples subjected to controlled conditions. The accuracy of the

27 prediction models was assessed on external samples (aged under known conditions)
28 through the cross correlation technique and the Root Mean Square Error (RMSE). The
29 models exhibited good collinearity for the aging temperature and the number of extrusion
30 cycles factors for all tested polymers, but not for the aging time factor. The RSME value
31 of the aging time factor was far from zero for all polymers. Plastic waste samples
32 provided analogous results; the aging time estimation was mostly negative in value. The
33 estimations of aging time and number of extrusion cycles were always positive in values,
34 where the most reasonable aging factor estimation was the number of extrusion cycles.

35
36
37 **Keywords:** FTNIR spectroscopy; polymer aging; polymer degradation; plastic waste;
38 prediction models

39 **1. Introduction**

40 Plastics have become an environmental challenge, even though they do not generally
41 possess a direct hazard to the environment. Their environmental footprint results from
42 the consumption of non-renewable resources, in addition to being non-degradable
43 (Sánchez and Collinson 2011). The extensive application of plastics creates a challenge
44 connected to the waste management of the related flows. Moreover, the fact that a
45 considerable fraction of the produced plastic is intended for single-use disposable
46 applications (Hopewell et al. 2009) and mainly in form of films for household and
47 industrial applications (Horodytska et al. 2018) exacerbates an already critical
48 framework. Municipal solid waste management integrated systems are generally defined
49 through the hierarchy of prevention, reuse, recycling, and recovery and disposal, in
50 decreasing order of priority (Denise Reike et al. 2018). The adoption of the circular-

51 economy concept on waste plastics compels the application of recycling activities (M.K.
52 Eriksen et al. 2018).

53 There are essentially four types of plastic recycling, categorized as primary (re-
54 extrusion), secondary (mechanical), tertiary (chemical recycling) and quaternary (energy
55 recovery) (Yu et al. 2016; Al-Salem et al. 2009). Mechanical recycling of plastics is most
56 appropriate when polymers are separately collected from contaminated source (Ragaert
57 et al. 2017). Chemical recycling represents processes able to recover synthesis
58 monomers or feedstock chemicals by depolymerization. Whereas quaternary recycling
59 or energy recovery is particularly utilized if plastics cannot be mechanically recycled or
60 re-extruded due to contamination, separation difficulties, or significant degradation
61 (Ragaert et al. 2017). This study focused on the mechanical recycling of plastics, since
62 this process is by far the most commonly applied at industrial level for material recovery
63 (Al-Salem et al. 2009). Generally, material's quality should be maintained during
64 reprocessing and use as a subsequent product; therefore mechanical recycling is often
65 limited to selected types of plastic wastes such as Polyethylene terephthalate (PET)
66 bottles (Barlow and Morgan, 2013). The recycling of other types of polymers can be
67 more complex, due to the wide variety of grades, poor recovery, cross-contamination,
68 and downgrading in quality (Hopewell et al. 2009). The common difficulties related to
69 mechanical recycling are the heterogeneity of plastic wastes and the deterioration in
70 polymers' properties due to use and aging (Brandrup 1996; Perugini et al. 2005; Ragaert
71 et al. 2017). Polymer degradation can cause changes in chemical, physical and
72 mechanical features (Beninia et al. 2011; Anne Shayene Campos de Bomfim et al.
73 2019). Polymeric surface can also be attacked by material weathering (temperature,
74 humidity and light), microorganisms and chemical solutions (Alassali et al. 2018a;

75 Picuno et al. 2019a; Picuno et al. 2019b). Polymer degradation; occurring due to thermal
76 oxidation mechanisms is the focus of this study, as these mechanisms are typically
77 activated when the polymer is exposed to environmental conditions as well as to
78 elevated temperatures (i.e. during extrusion), in presence of oxygen (Izdebska 2016). As
79 a consequence, integrating systems that are able to determine the material quality and
80 degree of degradation in the industrial recycling scheme could strongly improve the
81 recycling process.

82 In a previous study, Near Infrared (NIR) spectroscopy was employed to propose
83 polymers' degradation-prediction models, those able to predict plastic aging by focusing
84 on the degree of oxidation (Alassali et al. 2018b). NIR spectroscopy was chosen due to
85 its wide application in plastic sorting facilities (Huth-Fehre et al. 1995; Wahab et al.
86 2006; Masoumi et al. 2012; S. Brunner et al. 2015) and due to its fast, accurate, and
87 non-destructive features (Blanco and Villarroya 2002). This work is a follow-up to the
88 previously conducted study by (Alassali et al. 2018b) and it aims at validating the
89 generated models and their ability in predicting polymers' degree of thermal oxidation. In
90 details, the prediction capability of the generated models was verified by the cross-
91 validation technique (Pasquini 2003), a basic statistical technique used for estimating
92 the predictive performance of a model (Bishop 2006) that typically relies on a small
93 dataset (Goodfellow et al. 2016). In order to achieve the validation of the aging-
94 prediction models—generated for the polymers polypropylene (PP), low-density
95 polyethylene (LDPE), polyethylene terephthalate (PET), and acrylonitrile butadiene
96 styrene (ABS), discretely—four sets of samples of virgin polymers were aged under
97 controlled conditions. The applied aging method simulates environmental conditions, yet
98 accelerated. At molecular level, the thermo-oxidative degradation of the studied

99 polymers is a process accomplished with exposing the material to elevated
100 temperatures in the presence of oxygen (Song et al. 2014). Consequently, a variation in
101 the polymeric structure is provided as a result of compound's oxidation. The thermal
102 oxidation rate and extent of each polymer are unique, which generally depend on the
103 chemical structure and the stability of the polymeric chains (Alassali et al. 2018b). In this
104 study, virgin material (free of additives and stabilizers) was used. This was important to
105 decrease the number of variables in building the aging models. Certainly, different
106 additives, stabilizers and coloring agents may contribute to the degree of degradation
107 and hence to the generated mathematical models. However, this study focused on
108 evaluating the possibility of producing aging-prediction models, and re-applying them on
109 external samples (treated differently).

110 The second aim of this study was to utilize the validated age-prediction models to
111 forecast the degree of thermal oxidation (aging) of plastic waste samples (deriving from
112 e-waste) as well as on mechanically recycled samples, in order to test the viability of
113 implementing the models on industrial-scale for the purpose of material recovery for
114 recycling. To our knowledge this study is the first to investigate the reliability of non-
115 invasive age-predictive models on waste plastics. Compared to the previous study
116 (Alassali et al., 2018a), this work exhibits the following progresses: (I) a different and
117 more complex validation approach was adopted, (II) a significant factor (number of
118 extrusion cycles) was included to account for plastic aging by processing, and (III) the
119 generated models were tested on real waste samples (derived from waste electrical and
120 electronic equipment)

121

122 **2. Materials and Methods**

123 **2.1. Materials**

124 *2.1.1. Virgin plastic samples under controlled aging condition*

125 Virgin polymers (i.e. polymers free of additives) were either oven-aged under controlled
126 conditions—which means at defined temperature and duration (to simulate thermo-
127 oxidative effects)—or extruded (to simulate plastic mechanical processing) for the
128 purpose of validation. The same materials used in creating the aging models (Allassali et
129 al. 2018b) were also used for their cross-validation:







- 130 - cylindrical granules of ABS from POLYLAC PA-747 - CHI MEI CORPORATION;
- 131 - granules of PET, provided from NEOPET 82 FR - INEOS Olefins and Polymers
132 Europe;
- 133 - cylindrical granules of LD-PE, provided from INEOS Olefins and Polymers
134 Europe; and
- 135 - pellets of PP, provided from Olefins and Polymers Europe.





136
137 *2.1.2. Plastic waste samples*

138 The second set of samples was obtained from an e-waste collection point in the city of
139 Hamburg (Germany). Ten items of different brands were selected, and only their plastic
140 components were considered in this study (see Table 1). The polymers of each
141 component were identified as specified in section 2.5.2.

142 Table 1. Description of the plastic waste samples deriving from e-waste units

Identified in the	e-waste unit	Image	Color	Polymer
-------------------	--------------	-------	-------	---------

study as				type
PP-1	Lamp cup		White	PP
PP-2	Water container of coffee maker		Transparent	PP
PP-3	Base of coffee maker		White	PP
PP-4	Closure of a juicer		White	PP
PP-5	Water container of an iron		White to transparent	PP
PP-6	Inner part of an iron		White	PP

ABS-1	Hand mixer		White	ABS
ABS-2	Case of digital clock radio		White-yellowish	ABS
ABS-3	Router case		White	ABS
ABS-4	Router case		White	ABS

143

144 **2.2. Plastic aging-prediction models**

145 As was explained in (Alassali et al. 2018b), aging-prediction models were created
 146 utilizing the NIR spectra (obtained from a Bruker Optics FT-NIR spectrometer MPA,
 147 Multi-Purpose Analyzer) of differently aged virgin polymers.

148 As a first step, controlled thermal aging of the material was conducted in a BINDER

149 oven, where two aging factors were considered (i.e., temperature and time), to simulate
150 the thermo-oxidative degradation of plastics during their use in accordance with ASTM-
151 F1980-07. The plastic aging-prediction models were generated depending on the
152 relation between the experimental aging parameters (i.e., time (h) and temperature (°C))
153 and the NIR spectra. The NIR spectra of differently aged polymers exhibited specific
154 variations in the absorbance intensity, related to changes taking place in the materials
155 chemical structure due to oxidation, in other words degradation. This can be assumed
156 with confidence, since the material used to build the models is virgin, without any
157 additives and stabilizers. The dependent variable was the absorbance at a number of
158 wavelengths, while the independent variables were the properties identified for the
159 study: time of exposure and temperature. PLS (Partial Least Squares) chemometric
160 algorithm could derive the empirical spectroscopic models for each polymeric material
161 (PET, ABS, LDPE and PP) after being aged at different conditions. This procedure
162 simultaneously reduced the amount of the spectral data and tried to find a regression
163 over the data. The underlying basis for the models and putative mechanisms of oxidation
164 was based on the observed spectral changes and by applying the principal component
165 analysis (PCA). After collecting the spectra, the modelling procedure was realized using
166 OPUS software. The “Quant 2 Method” option was used to apply a PLS regression on
167 the data points, where the aging parameters were inserted in relation to the NIR spectra
168 by the operator. Furthermore, the models were optimized through processing the data
169 points by the software OPUS to enhance the data fitting. The processing included data
170 pre-treatment. The different pre-treatment methods were semi-automatically selected,
171 where the PLS model (created by OPUS) provided suggestions (by proposing data
172 treatment methods and selecting regions of wavenumbers), after which, the operator

173 optimized the selection based on the obtained statistical evaluation. As a result, and due
174 to considering two aging factors, two linear models for every polymer were generated;
175 estimated aging time (h) and aging temperature (°C) of each sample could be obtained
176 by mathematical relations.

177 To get one linear relation between model-predicted parameters and experimental
178 parameters, thermo-oxidative aging time was calculated following Equation (1); once
179 applying the model-predicted aging parameters and a second time applying the
180 experimental aging parameters, finally they were plotted against each other. Thermo-
181 oxidative aging was calculated applying the concepts of chemical reaction kinetics
182 (Murray et al. 2013). It was assumed that the accelerated thermo-oxidative aging roughly
183 corresponds to doubling the aging rate for each increase of 10 °C (Shimada and Kabuki
184 1968; Boldizar and Möller 2003), hence, a Q10 value of 2 was used in Equation (1)
185 (Mandal et al. 2014; Alassali et al. 2018b; Alassali et al. 2018a). This relation is polymer
186 dependent; hence different models are expected to be obtained for different polymers.

$$187 \quad t_{(accelerated)} = t_{real} \times Q10^{(T_{aging} - T_{ambient})/10} \quad (1)$$

188 Where,

189 $t_{(accelerated)}$: accelerated aging time (in days),

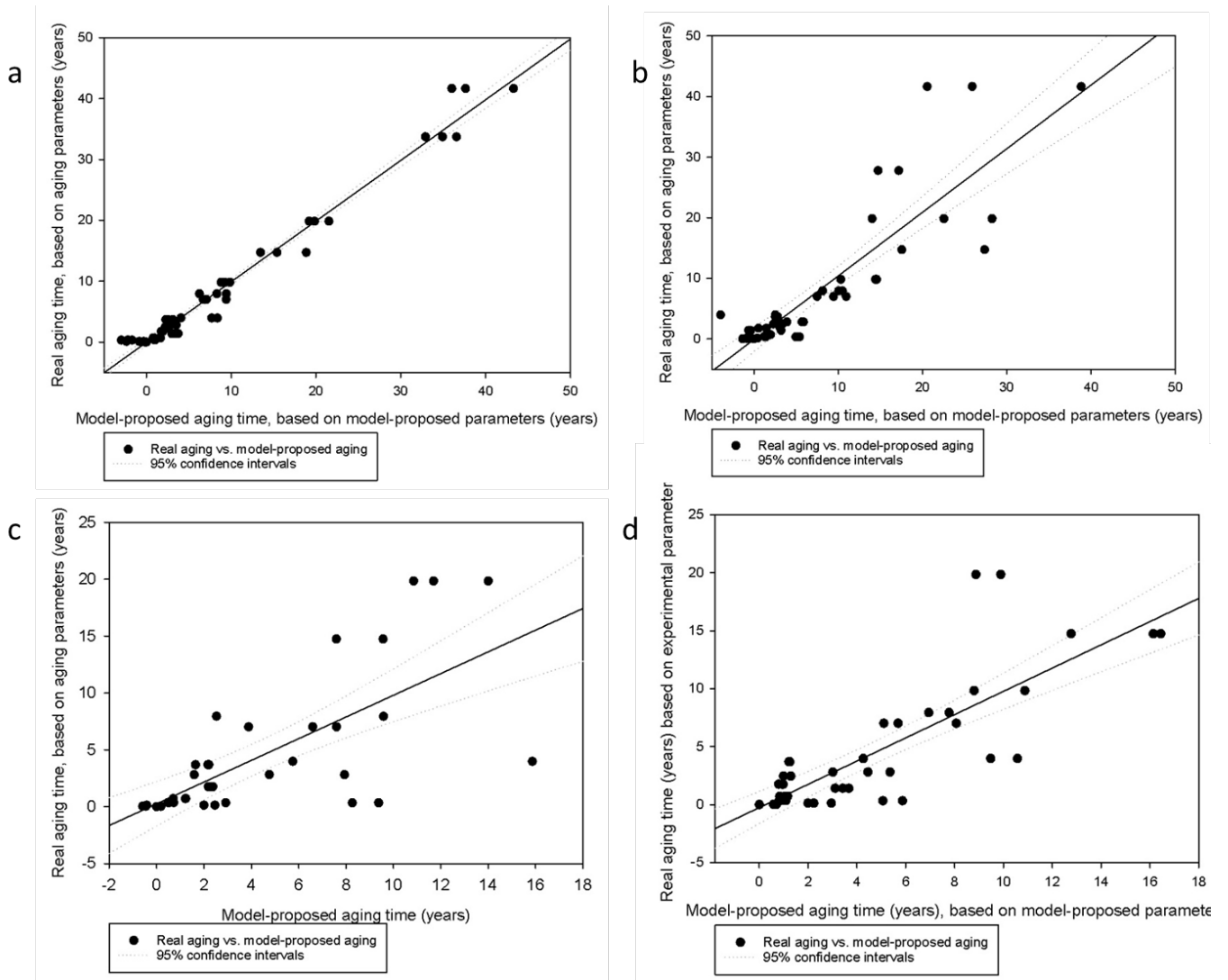
190 $t_{(real)}$: the real aging time applied, using accelerated conditions (in days),

191 Q10: accelerated aging factor (here 2 is considered (Murray et al. 2013)),

192 $T_{(aging)}$: the aging temperature applied in the treatment process (°C),

193 $T_{(ambient)}$: the ambient temperature (°C).

194 The aging-prediction models explained in (Alassali et al. 2018b) (see Figure 1) were
195 used in this study with the aim of cross-validation (Equations 2-5), by predicting real (i.e.
196 experimental) aging parameters from the provided model-proposed aging parameters.



198

199 Figure 1. Calculated real aging time versus calculated model-proposed aging time: (a)

200 ABS, (b) PET, (c) PP and (d) PE (Alassali et al. 2018b).

201

202 $ABS: Real\ ageing = 0.9961 \times Model\ predicted\ aging - 0.023$ (2)

203 $PET: Real\ ageing = 1.049 \times Model\ predicted\ aging - 0.0771$ (3)

204 $PP: Real\ ageing = 1.0832 \times Model\ predicted\ aging - 0.341$ (4)

205 $PE: Real\ ageing = 1.0016 \times Model\ predicted\ aging - 0.251$ (5)

206

207

208 **2.3. Description of the models' validation technique**

209 The objective of validating the generated NIR-based aging models, as any other
210 analytical procedure, is to demonstrate that it is suitable for its intended purpose (Broad
211 et al. 2002). Hence, the accuracy of the generated models needed to be evaluated (Pojić
212 et al. 2012), in this case by measuring how well the NIR prediction value match a given
213 reference value that is experimentally obtained. In many applications based on statistical
214 analysis, cross-validation is one of the simplest and most commonly reproduced
215 methods for estimating the prediction accuracy, therefore the error of a model (Hastie et
216 al. 2009). Given a specific and sufficiently large set of data, a fraction of the dataset
217 could theoretically be used for building the model, whereas the other part of the dataset
218 could be utilized as a validation test set. Moreover, there is another method for cross-
219 validation, which is called leave one out cross-validation (Öğütçü et al. 2012). However,
220 it is often the case in studies, like the present one, where the dataset is not big enough
221 to allow for its splitting. In order to overcome this issue and still be able to validate the
222 models in this study, the following 6-steps validation technique was applied to test the
223 models' accuracy:

- 224 1. The models to be validated were identified and equations describing each model
225 were derived (Equations 2-5);
- 226 2. New, independent sample sets of virgin and pure material were assimilated by the
227 application of thermal aging under defined conditions;
- 228 3. The newly created independent test sets were cross-validated with the before
229 generated PLS aging-prediction models;

- 230 4. The OPUS software was used to transform the NIR spectra into numerical values;
- 231 5. The model-proposed parameters were used to calculate the real aging
- 232 parameters following the linear mathematical relation created for age-prediction
- 233 (Equation 2-5);
- 234 6. The real aging parameters (as were calculated in step 5) were compared to
- 235 experimental aging parameters (applied in the lab) and the accuracy was
- 236 statistically tested.

237 The above-mentioned steps are described in detail in section 2.4.

238

239 **2.4. Model's accuracy statistical evaluation by cross-validation**

240 A test set of pure samples was acquired for each material by applying specific aging

241 temperature and aging time in a BINDER oven, as described in Table A in the

242 supplementary data. The test samples were analyzed through a Bruker Optics Fourier

243 Transform near infrared (FT-NIR) spectrometer MPA (Multi-Purpose Analyzer) and

244 acquired spectra were further processed and analyzed with OPUS spectroscopy

245 software from Bruker. The spectra of each test sample (described in Table A) were

246 cross validated with the corresponding aging models resulting in model-proposed aging

247 time (h) and model-proposed aging temperature (°C). Equation (1) was applied to

248 combine both parameters to calculate the model-proposed thermo-oxidative aging time

249 (expressed in years). The real thermo-oxidative aging time values for each polymer

250 were then calculated following the Equations 2, 3, 4 and 5 respectively, which results

251 were compared to the thermo-oxidative aging time calculated from the experimental

252 parameters (see the data repository, Table A) to calculate the models' aging-prediction
253 accuracy.

254 The accuracy of age prediction was assessed by calculating the mean error (ME) and
255 mean square error (MSE) (Prestwich et al. 2014; Azadi and Karimi-Jashni 2016), shown
256 in Equation (6) and Equation (7), respectively.

$$257 \quad ME = \frac{1}{n} \sum_{i=1}^n (y'_i - y_i) \quad (6)$$

$$258 \quad MSE = \frac{1}{n} \sum_{i=1}^n (y'_i - y_i)^2 \quad (7)$$

259 Furthermore, the Root Mean Square Error of Cross-Validation (RMSECV) (Equation (8))
260 (Chai and Draxler 2014)) was calculated for the test samples to characterize the model's
261 prediction accuracy.

$$262 \quad RMSECV = \sqrt{\frac{\sum_{i=1}^n (y'_i - y_i)^2}{n}} \quad (8)$$

263 where:

264 y_i = real thermo-oxidative aging time (using experimental values)

265 y'_i = real thermo-oxidative aging time estimated by the generated model

266 n = number of data points

267

268 **2.5. Creating a global polymer aging-prediction model**

269 *2.5.1. Including the extrusion effect in the polymer thermo-oxidative aging model*

270 Mechanical recycling of post-consumer plastics consists of sorting the material by
271 polymer type and color, shredding, washing, drying, possibly sorting once more the
272 resulting flakes and then extruding them in order to be transformed into granules. The
273 generated granules can be further molded to form specific consumer products. In the

274 context of this research, three extrusion cycles were performed. The first extrusion cycle
275 of virgin granules represented the first production process. The second extrusion cycle
276 was considered as a first recycling cycle, and the third extrusion resembled a second
277 cycle of recycling. Mechanical extrusion was performed using HAAKE™ Rheomex CTW
278 100 OS Twin Screw Extruder.

279 First, the abovementioned models were applied to predict the age of extruded samples
280 to evaluate for the possibility of using the same models to predict the age (degree of
281 oxidation) of extruded polymers. As the models failed to efficiently and reproducibly
282 predict material aging after being extruded, new aging models were built, this time
283 including three parameters instead of two: heating temperature (°C), heating time (h)
284 and the number of extrusion cycles. These three parameters could not be combined in
285 one equation, therefore Equation (1) was not utilized and a model for each parameter
286 was independently built.

287

288 *2.5.2. The application of the global aging-prediction models to forecast the*
289 *degree of waste material oxidation*

290 Plastic samples originated from e-waste were identified, sorted and separately shredded
291 by a Retsch Cutting Mill SM 300 to a size below 4.0 mm. The shredded samples were
292 analyzed by Bruker Optics FT-NIR spectrometer and acquired spectra were further
293 processed and analyzed with OPUS spectroscopy software. The spectra were cross
294 validated with the corresponding aging models, where a model-predicted aging time (h),
295 aging temperature (°C) and number of extrusion cycles for each test sample were
296 respectively provided.

297 **3. Results and Discussion**

298 After aging, changes in the chemical structure were observed, identified by changes in
299 the absorbance intensity of the NIR spectra of differently aged polymers. Multivariate
300 calibration algorithms like PLS correlate spectral intensity (absorbance values) in
301 specified wavelength regions with experimentally obtained aging parameters (time and
302 temperature in this study). The calibration work, entirely achieved by Quant 2 Method.
303 The results were obtained as data points; provided value of the parameter of interest
304 versus the model-predicted value. The applied relation was PLS, hence, the data points
305 generated a linear mathematical relation (shown in Figure 1 and Equations 2-5). For the
306 cross-validation, the method developed to generate the models was retrieved and the
307 spectral data of the test samples were automatically processed (every polymer was
308 separately processed by its own mathematical relation). The software returned values of
309 respective aging parameters, as the model estimates. The model-predicted values were
310 plotted against the real values; this is presented in Figures 2 (a, c) and 3 (a, c), as black
311 stars. The deviation between the plotted test values and model's relation (Figures 2 (a,
312 c) and 3 (a, c), grey circles) could give a quantifiable evaluation of the prediction
313 accuracy.

314 **3.1. Aging time and temperature effects on the calculated thermo-oxidative** 315 **aging**

316 Thermo-oxidative degradation becomes increasingly important as the exposure
317 temperature and time increase, delivering distinctive changes for each polymer.

318 Overall, the model-predicted thermo-oxidative aging time increased by increasing each

319 of the applied aging factors. For all models, the model-predicted aging temperature ($^{\circ}\text{C}$)
320 was more accurately estimated than the model-predicted aging time (h). Moreover, at
321 higher aging temperatures, the thermo-oxidative aging rate increased more significantly
322 by increasing the experimental aging time. Simultaneously, the aging-prediction
323 accuracy decreased when elevated temperatures were applied, as was indicated by the
324 calculated RMSE values, especially for PET, PP and PE. The higher the RMSE value,
325 the lower the model's accuracy. For PET, RMSE increased from 0.98 for samples aged
326 at 85°C to 9.01 for samples treated at 120°C , for PP, RMSE increased from 0.85 for
327 samples aged at 85°C to 6.51 for samples treated at 120°C and PE it increased from
328 1.15 for samples treated at 85°C to 6.21 for samples treated at 120°C . This indicates
329 that the prediction accuracy decreases at higher aging temperatures, which could be
330 attributed to the non-linear effect of elevated temperatures on the degradation rate of the
331 tested polymers, where PLS method was assumed.

332 **3.2. Aging models' accuracy assessment by cross-validation**

333 *3.2.1. ABS*

334 Figure 2.a shows an accurate estimation of the model-predicted thermo-oxidative aging
335 time of ABS (MSE = 0.90) at an experimental thermo-oxidative age lower than 5 years.
336 Yet, the overall age-prediction accuracy of the selected sample-set showed a slight
337 decrease (MSE = 2.42), which was due to the impreciseness in age estimation for the
338 sample treated at 120°C for 336 h, possibly due to range of material coloration. Cross-
339 validation was performed by calculating the thermo-oxidative aging time twice:

- 340 (I) Using the experimental aging parameters (i.e., time and temperature);
- 341 (II) Using the model's estimated aging parameters to calculate relevant real aging

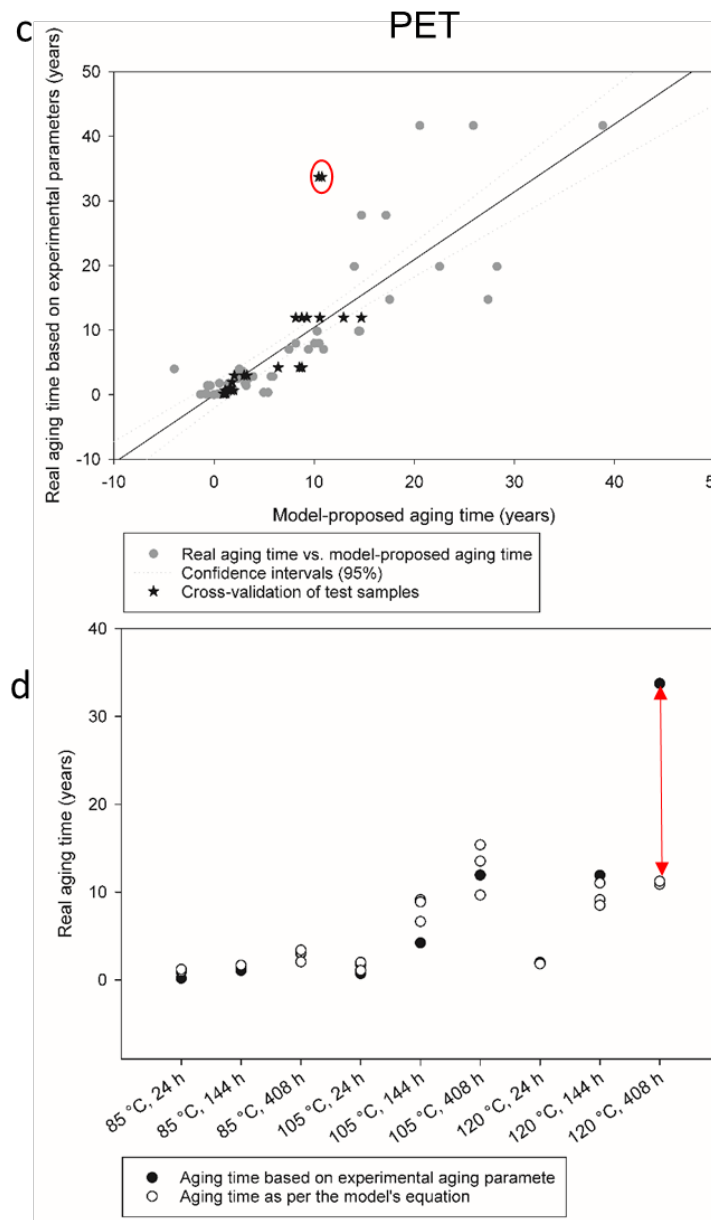
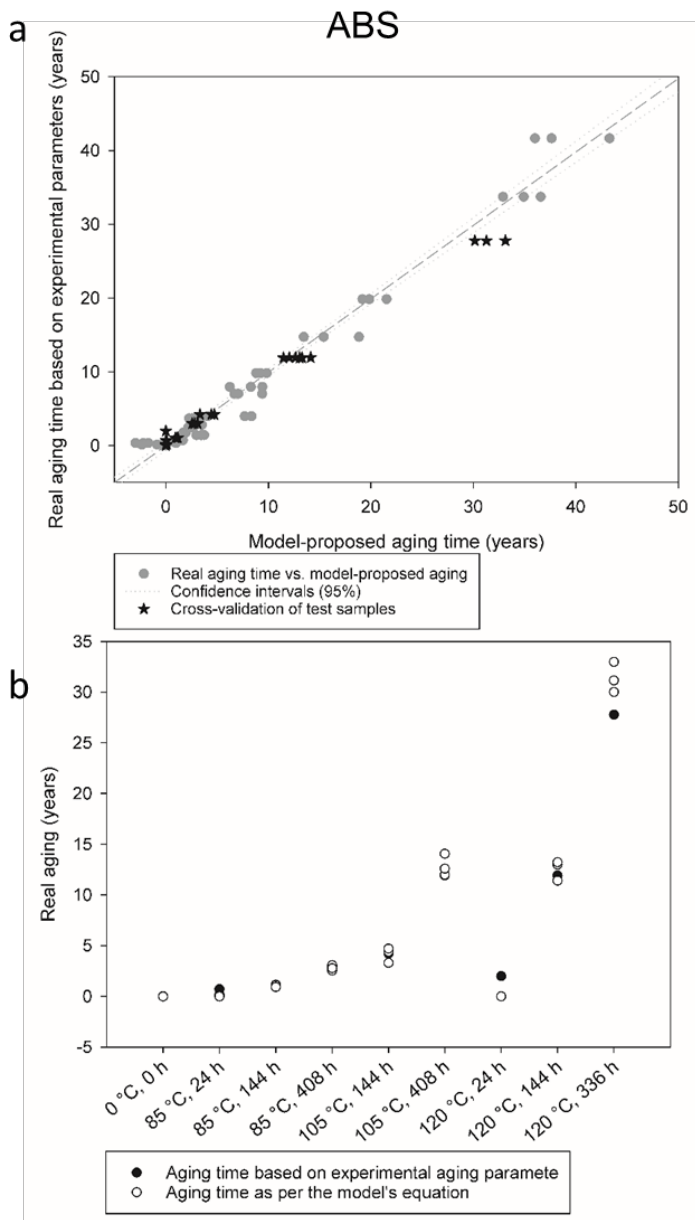
342 time (applying Equation (2); $y = 0.9961 x + 0.023$).

343 Values obtained from (I) and (II) were simultaneously plotted (see Figure 2.b). There is a
344 robust consistency in the values; they were generally overlapping. For the material aged
345 at 120 °C for 336 hours, the calculated model-based thermo-oxidative aging time was
346 higher by ~2 years for one sample and by ~4 years for another, indicating a range of
347 variation, yet less than what was observed by the rest of tested polymers. This variation
348 could be attributed to the possible non-linear oxidation behavior of the material, which
349 was interpreted by linear regression methods. The bias of the values was however
350 negligible (i.e., ME = 0.21). The overall RMSECV value (i.e., 1.51) shows a good age
351 estimation model.

352 3.2.2. PET

353 The cross-validation conducted on PET test samples indicated more compliance in the
354 aging region ≤ 11 years; model-predicted aging time varied for samples exposed to
355 thermo-oxidative aging parameters simulating aging time higher than 11 years (see
356 Figure 2.c). A high range of error between experimental thermo-oxidative aging time and
357 model-predicted thermo-oxidative aging time was obtained for the material aged at 120
358 °C for 408 h. The thermo-oxidative aging time calculated from the model's calibration
359 equation ($y = 1.049 x - 0.0771$ for PET) was plotted together with the real thermo-
360 oxidative aging time (calculated as per experimental parameters) to measure the degree
361 of agreement (see Figure 3.d). At aging temperature of 85 °C, the model showed high
362 prediction accuracy for all tested aging duration (bias values ranging between -0.94 and
363 1.01 only). For the thermo-oxidative aging at 120 °C, the aging time prediction accuracy
364 had an inverse relationship with the aging duration, where it was the lowest for the

365 material treated at 120 °C for 408 h. Generally, it was observed that the age prediction
366 accuracy decreased with increasing the severity of aging (see Figure 2.d). When the
367 samples treated at 120 °C for 408 h were excluded, the cross-validation of the PET
368 aging model provided high accuracy, with ME value of 0.64 and MSE value of 4.48. Yet,
369 the age-prediction accuracy of the PET aging model decreased significantly by cross-
370 validating the mentioned sample; the MSE increased to 46.96, with an overall cross-
371 validation RMSE value of 6.85. As well, this could be explained by the stability of PET
372 under the applied aging conditions, which did not result in a linear aging behavior as
373 estimated.



374
 375 Figure 2. Left (a, b) for ABS and right (c, d) for PET: (a, c) Test samples cross-validated
 376 with the aging model, (b, d) comparison between real thermo-oxidative aging time
 377 obtained from experimental parameters and real thermo-oxidative aging time obtained
 378 from the generated regression model.

379 **3.2.3. PP**

380 The PP aging model had a low collinearity, $R^2 = 0.64$ (see Figure 1 and Equation (4)),

381 yet this value was sufficient for a screening with wider error intervals (Krapf 2013). As
382 shown in Figure 3.a, higher aging-prediction accuracy of the test samples was obtained
383 for those that underwent short thermo-oxidative aging period (≤ 2 years). The real
384 thermo-oxidative aging of test samples was frequently accurately predicted applying the
385 model's formula ($y = 1.083 x - 0.341$), except for samples treated at 120 °C (see Figure
386 3.b). The MSE of the cross-validation for all samples treated at 85 °C and 105 °C was
387 2.0, which increased by about 6 folds when the samples treated at 120 °C were included
388 (i.e., MES value reached 11.83). This indicates that with increasing the severity of the
389 treatment, age-prediction accuracy decreases, while the effect of aging temperature was
390 more significant than the aging time. The overall cross-validation RMSE (3.44) value is
391 yet acceptable.

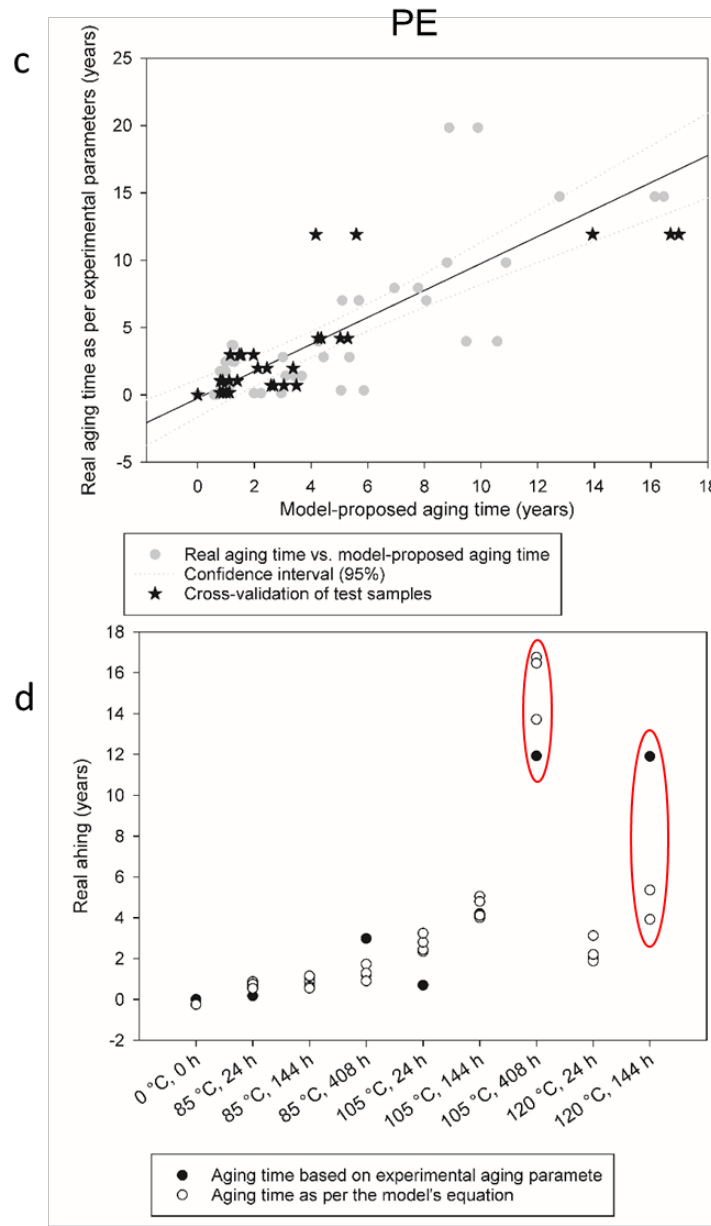
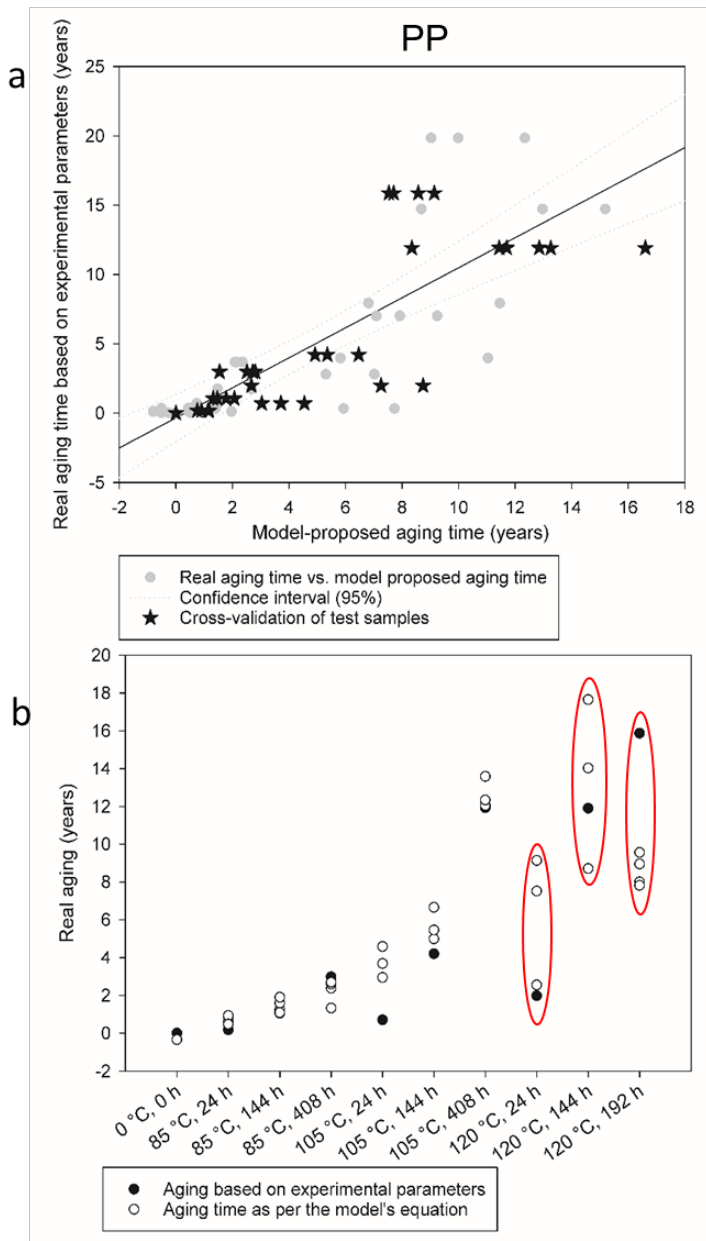
392

393 3.2.4. PE

394 As indicated in Figure 1 and Equation (5), the collinearity of the relation between
395 experimental thermo-oxidative aging time and model-predicted thermo-oxidative aging
396 was relatively low for PE (i.e., 0.66). However, the PE aging model in comparison to real
397 aging data showed good model estimation, with wider range of prediction error. As
398 shown in Figure 3.c, the cross-validation of test samples falls in the region of model's
399 confidence interval, except for the samples aged at 105 °C for 408 h and at 120 °C for
400 144 h, where the calculated thermo-oxidative aging for both conditions, applying
401 Equation (1), is 11.9 years. The model's anticipated aging was overestimated (by 2 to 5
402 years) for the samples aged at 105 °C for 408 h, where an age underestimation (by 6 to
403 8 years) was provided by the PE aging model for the samples aged at 120 °C for 144 h.

404 Following the regression model generated formula ($y = 1.016 x - 0.251$), the calculated
405 real thermo-oxidative aging time showed negligible variations in comparison to the
406 experimental thermo-oxidative aging time for all test points, except for the above
407 mentioned two samples (see Figure 3.d). The overall cross-validation ME was
408 insignificant (i.e., 0.0182), yet the overall age-prediction accuracy was lower than what
409 was provided by the ABS aging model (MSE of 6.01). The calculated RMSE value for
410 the cross-validated samples indicated higher oxidation-prediction accuracy (i.e., 2.45) in
411 comparison to PET and PP aging models.

412



413
 414 Figure 3. Left (a, b) for PP and right (c, d) for PE: (a, c) test samples cross-validated with
 415 the aging model, (b, d) comparison between real thermo-oxidative aging time obtained
 416 from experimental parameters and real thermo-oxidative aging time obtained from the
 417 generated regression model.

418
 419

420 **3.3. Comparison of the quality of the aging-prediction models**

421 The aging-prediction models of different polymers (i.e., ABS, PET, PP and PE) were
422 assessed by calculating the RMSECV of the test sets described in Table A in the
423 supplementary material, which is calculated by weighing the deviation of the
424 experimental thermo-oxidative aging values from the model's calculated thermo-
425 oxidative aging time (using the created regression models in Figure 1). The RMSECV
426 value calculated for the ABS aging model (1.51) was lower than the values calculated
427 for PE and PP aging models (2.45 and 3.44, respectively), while the highest value was
428 obtained for PET aging model (6.85). These results indicated that the performed cross-
429 validation provided the best fitting for ABS aging model, however the model's quality
430 decreased for other polymers aging models, to be the lowest for the PET aging model.
431 Degradation process occurs due to the influence of thermal, chemical, mechanical,
432 radiative and biochemical factors; resulting in deterioration of mechanical and physical
433 properties of polymers. The degradation occurs due to changes in the main backbone or
434 side groups of the polymer (Venkatachalam et al. 2012). The degradation of PE and PP
435 could result in chain breakage and formation of radicals, which are easily oxidized.
436 Therefore, it is expected to obtain an increase in C=C, C=O or C—OH bonds in the
437 generated NIR spectra after material aging, in addition to the increase in the
438 concentration of methyl groups (Alassali et al. 2018b). However, the models indicated
439 that the oxidation rate of PE and PP is slower than what the model would predict, which
440 resulted in low collinearity and reduced age estimation accuracy. In PET, the aromatic
441 ring connected to a short aliphatic chain provides stiffness to the molecule. The lack of
442 segmental mobility in the polymer chains results in relatively high thermal stability

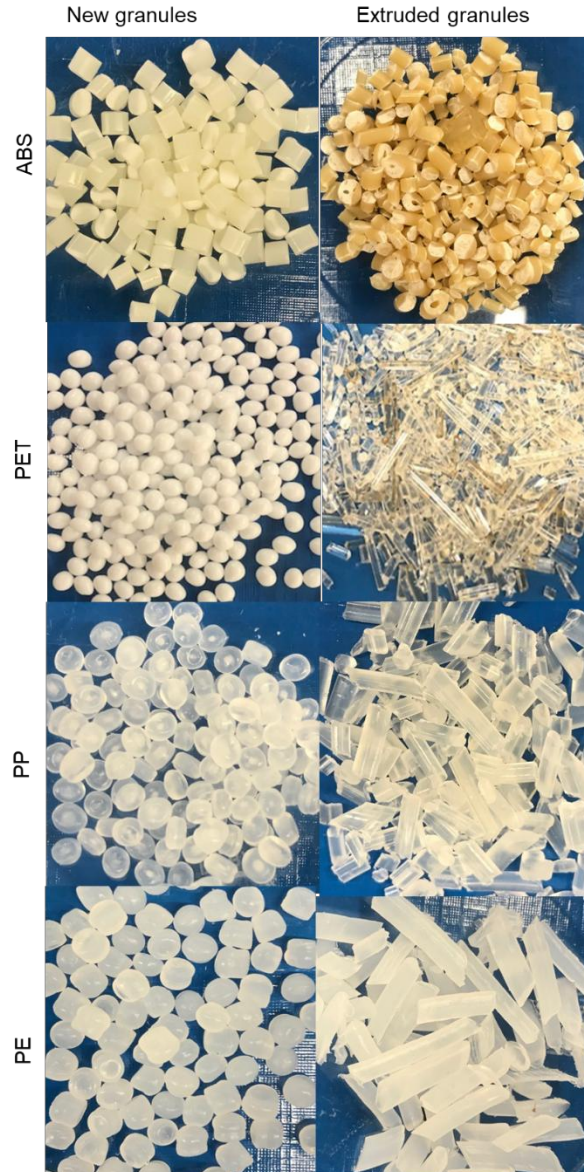
443 (Venkatachalam et al. 2012). Nevertheless, the thermal degradation of PET was
444 reported to take place leading to cyclic oligomers and chain scission, resulting in vinyl
445 ester and acid end-groups (Holland and Hay 2002). As per the generated aging
446 prediction model for PET, the model aging time and aging temperature estimation had a
447 range of values, providing that the chemical stability of the polymer resulted in
448 inhomogeneous degradation performance. On the other hand, degradation of the
449 elastomeric polybutadiene phase (i.e., containing C=C) in ABS is initiated by hydrogen
450 abstraction from the carbon α to unsaturated bonds, resulting in hydroperoxide radicals
451 and producing carbonyl and hydroxyl products. Furthermore, degradation of the
452 styrene–acrylonitrile phase in ABS takes also place by thermo-oxidative degradation, yet
453 in lower rate (Tiganis et al. 2002a). Generally, the age-prediction model of ABS showed
454 a high accuracy and optimized linearity, which is attributed to the linear relation between
455 the degree of degradation of the polymer and the aging severity, which fits with the
456 linear regression methods being applied.

457 Comparing the RMSECV values of the test samples to what was obtained by the original
458 aging model described by (Alassali et al. 2018b), lower values were obtained for ABS,
459 PE and PP, whereas it was higher for PET. This could be attributed to the limited
460 number of test samples used in the cross-validation in comparison to the data points
461 used in constructing the models; having few samples, which were unable to capture the
462 model's trend, allowed for an elevated RMSECV value. Despite the bias in the predicted
463 thermo-oxidative aging time, the four models were able to provide an age estimation
464 tool.

465 **3.4. The application of the original age-prediction models as a tool of age**
466 **estimation of polymer samples**

467 3.4.1. *Extruded samples*

468 The utilization of the age-prediction models was incompatible to predict degradation
469 (i.e., aging) of extruded samples. As shown in the data repository, Table B, the predicted
470 aging parameters were below zero, especially for ABS and PET. This was attributed to
471 the great change in color of these two polymers after extrusion (see Figure 4).



472

473

Figure 4. The change of color of polymers after extrusion

474

3.4.2. Waste samples

475

As the data in the data repository, Table B showed, the model predicted negative aging

476

temperatures for samples PP-2 and PP-5 (from Table 1), which resulted in a negative

477

thermo-oxidative aging time (years) estimation. The predicted aging temperature of PP-

478

1, PP-3, PP-4 and PP-6 was too high (above 1000 °C), which resulted in an aging time

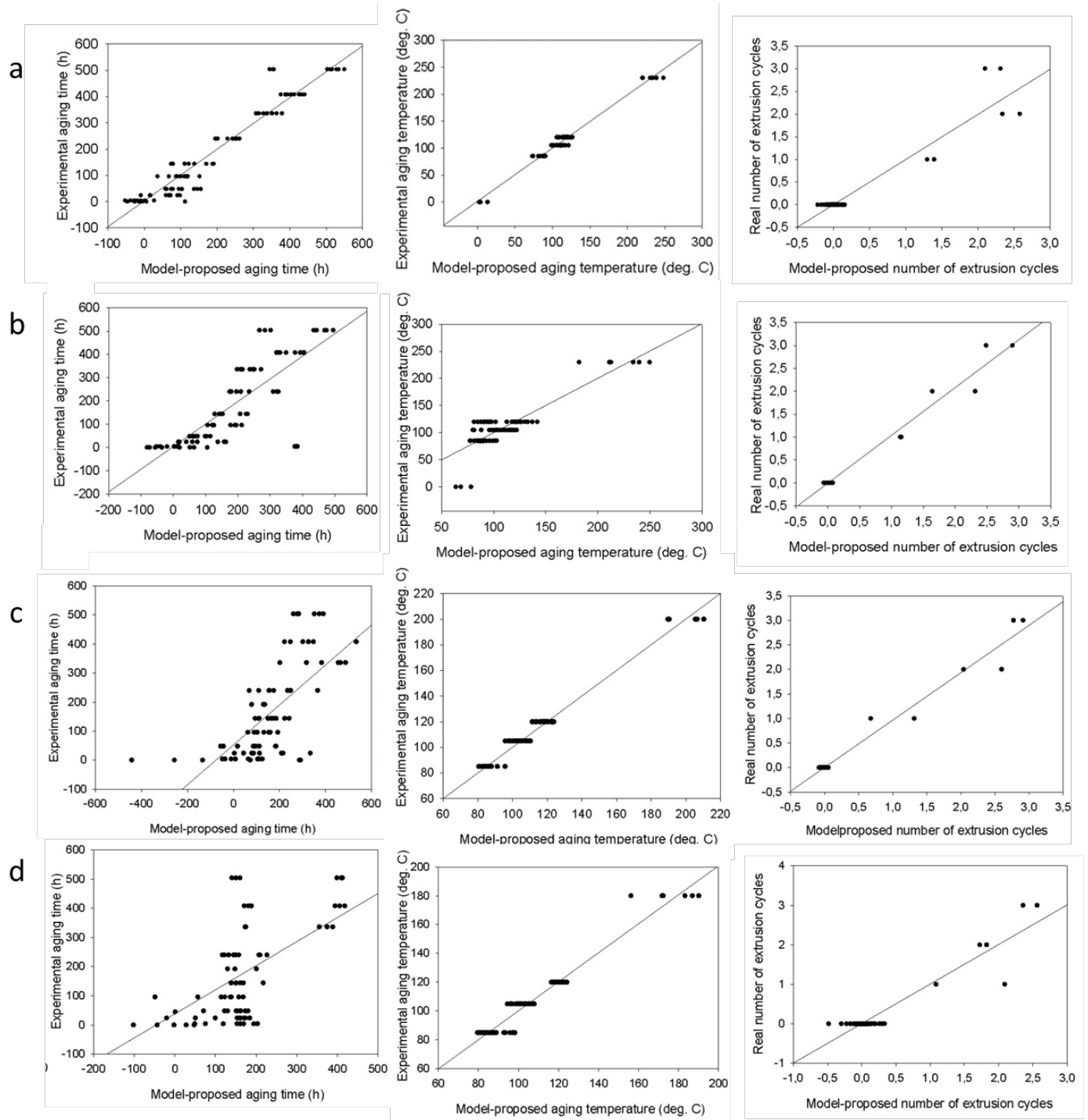
479

overestimation, especially for PP-6. This could be attributed to the effect of extrusion

480 and molding taking place during production, which has accelerated the thermo-oxidation
481 of the polymers and consequently resulted in intense coloration. For ABS, the aging
482 temperature of the material was mostly estimated to be negative, resulting in negative
483 values of thermo-oxidative aging time (years). The results support what was obtained in
484 extruded samples, where the granules color changes significantly by extrusion and
485 possibly molding. Not to forget the possible impact of stabilizers and antioxidants in the
486 plastics formulations to provide protection during processing or fabrication into finished
487 product (Dopico-García et al. 2011).

488 **3.5. Building a global polymer aging model**

489 In previous models, the effects of aging time and temperature were accounted.
490 However, in the production phase, polymers undergo harsher processing conditions,
491 where melting takes place during both, extrusion and molding. For this reason, the initial
492 models (including time and temperature factors) did not have the capacity to properly
493 predict thermo-oxidative behavior of consumer products (plastics derived from electrical
494 waste). Hence, the factor of number of extrusion cycles was additionally evaluated. For
495 this study, the number of extrusion cycles was restricted to 3. As can be seen in Figure
496 5, for each material (i.e., (a) ABS, (b) PET, (c) PP and (d) PE), three equations were
497 extracted, one to predict the aging time (h), a second one to predict the aging
498 temperature (°C) and a third one to predict the number of extrusion cycles (from left to
499 right in Figure 5).

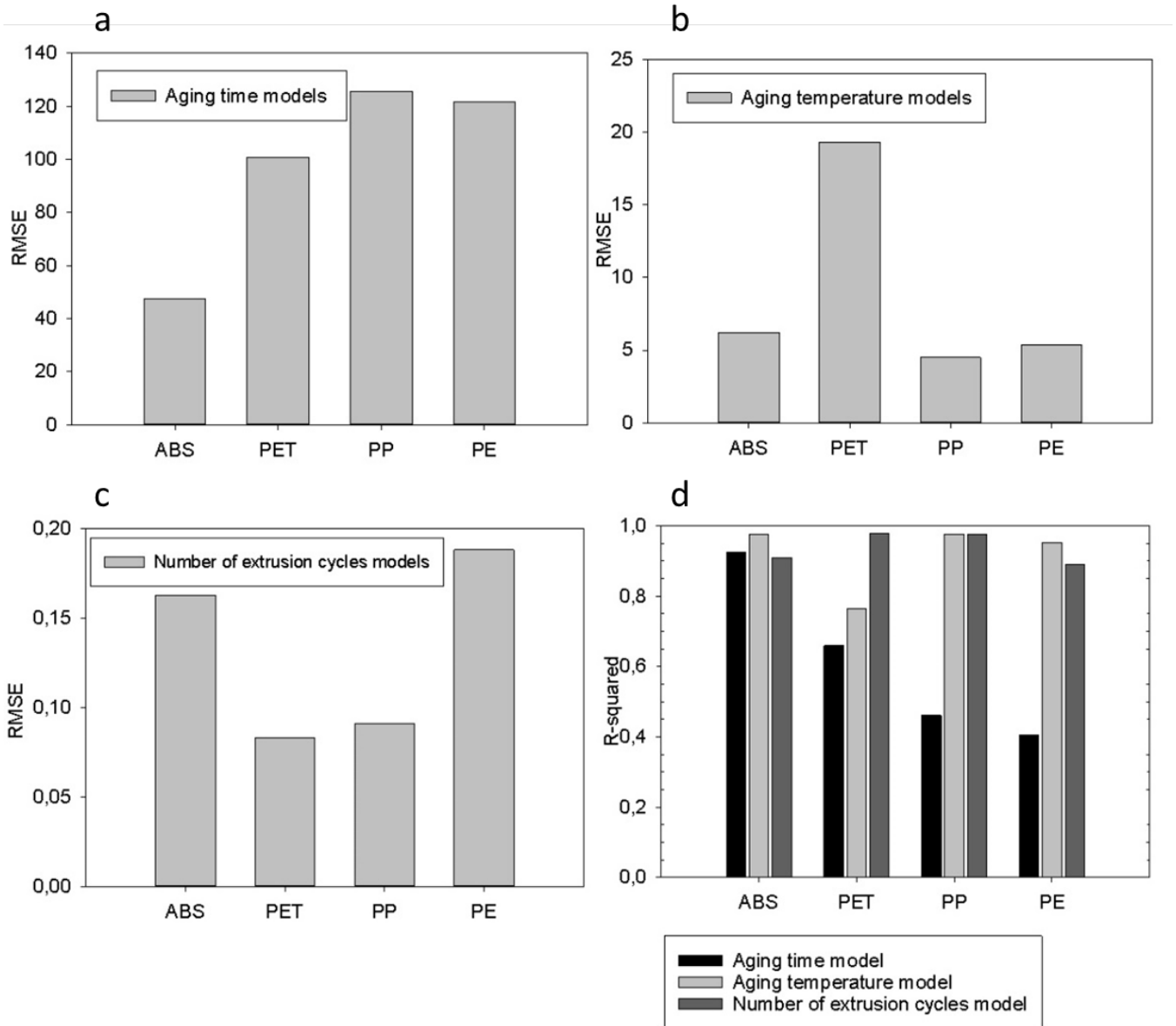


500

501 Figure 5. The global aging models created to predict materials' aging time (h), aging
 502 temperature ($^{\circ}\text{C}$) and number of extrusion cycles (from left to right) for (a) ABS, (b) PET,
 503 (c) PP and (d) PE.

504 The generated models were evaluated by calculating the RMSE for each aging
505 parameter, which was calculated by accounting for the difference between the model-
506 proposed value and the experimental value for virgin test samples. The model
507 constructed for ABS was the most efficient in comparison to PET, PP and PE (see
508 Figure 6). The model was less accurate in estimating the aging time (h) in comparison to
509 all other parameters (components), for all tested materials (ABS, PET, PP and PE). The
510 RMSE value was, however, the lowest for ABS (47.48) and the highest for PP (125.56)
511 (Figure 6.a). Aging temperature prediction was significantly more precise for ABS, PP
512 and PE, where the RMSE of the PET model showed a significant increase (lowering the
513 model's estimation accuracy) (Figure 6.b). For all tested polymers, the estimation of the
514 number of extrusion cycles was considerably accurate (see Figure 6.c). This could be
515 attributed to the limited number of extrusion cycles applied (ranging from 0 to 3).
516 Moreover, the R^2 value was calculated for all parameters of the global aging models
517 (see Figure 6.d). For ABS the relation between experimental aging parameters and
518 model-proposed aging parameters was mostly collinear (i.e., 0.92 for aging time
519 component, 0.98 for aging temperature component and 0.91 for number of extrusion
520 cycles component). The collinearity of the relation between real aging time and model-
521 proposed aging time for PET was relatively low (0.66), yet allowing for the application of
522 approximate calibration (Krapf 2013). The R^2 value increased significantly for the
523 extrusion cycle component for the PET global aging model to reach 0.98. For PP and
524 PE, the global aging model indicated poor aging time estimation, the R^2 values for the
525 aging time component for PP and PE were 0.46 and 0.40, respectively. Yet, for the
526 aging temperature component and number of extrusion cycles components, the R^2
527 values were both 0.98 for PP, indicating the model's applicability. The R^2 values were

528 similarly high for PE (i.e., for aging temperature component: 0.95 and for number of
 529 extrusion cycles component: 0.90), allowing for the application of the model for different
 530 purposes, covering quality insurance applications.



531
 532 Figure 6. Evaluation of the global aging models for ABS, PET, PP and PE; (a) RMSE for
 533 the aging time component, (b) RMSE for the aging temperature component, (c) RMSE

534 for the number of extrusion cycles component and (d) R^2 -value for the three mentioned
535 components of the aging models.

536 *3.5.1. The application of the global models to estimate the age of waste samples*

537 The aim of creating global aging models is to develop a quality control tool to assess the
538 quality of the recycling input material and, therefore, to improve the quality of recycled
539 material. The model-proposed aging time, aging temperature and number of extrusion
540 cycles were used to calculate the real aging time, aging temperature and number of
541 extrusion cycles following the equations provided by the generated global models. It can
542 be clearly seen from Table C (in supplementary material) that the models failed to
543 estimate the aging duration of the material, where values were either below zero
544 (especially for ABS polymer) or too high (PP-4 and PP-6). The predicted aging
545 temperature for ABS was 3 to 5 folds higher than that for PP, which is ascribed to the
546 material coloration. The estimation of the number of extrusion cycles for both materials
547 was reasonably acceptable; positive values in acceptable ranges were obtained.

548 **3.6. Economic and environmental considerations**

549 This research has significant practical, economic and environmental consequences. Life
550 Cycle Analysis assessed the environmental benefits of plastic recycling, compared to
551 disposal in waste-to-energy facilities, and results were controversial (Huysveld et al.
552 2019; Faraca et al. 2019; Khoo 2019). Considering the economic outcomes, plastic
553 recycling could easily become economically too expensive (if the recycled product
554 exhibits low features and consequently low market value) to achieve a net benefit
555 compared to disposal. However, as a general statement, policy interventions supporting

556 plastics recycling, as well as technological changes and a transparent communication
557 and collaboration between all stakeholders are needed to enhance the recycling process
558 (Hahladakis and Iacovidou 2019). Nowadays, recycling is usually associated with higher
559 economic efforts than incineration due to higher labor needs and enhanced transport
560 and sorting costs, hence, proposing an available technique (NIR sorting) in order to
561 enhance the quality of plastic recycling should be of a great significance in industrial
562 applications.

563 **4. Conclusions**

564 The aim of this study was to validate plastic aging-prediction models for their industrial
565 applicability, especially for material quality identification for recycling. A recent study
566 (Faraca et al. 2019) proved that if high quality of the recycled plastic is achieved, both
567 environmental savings and financial revenues are possible. Therefore the here
568 presented aging-prediction models could be of great help for material quality
569 identification in plastic sorting facilities.

570 The generated models showed effectiveness in age-estimation of experimentally aged
571 polymers. The ABS aging-prediction model was the most accurate among all tested
572 polymers, which was attributed to the quantifiable changes in the chemical structure
573 through aging. For other polymers (i.e., PET, PP and PE), although the accuracy of age-
574 estimation was lower, the models could still be applicable to estimate the age of
575 material, which was aged under controlled conditions. The original aging-prediction
576 models provided negative aging values for extruded ABS and PET samples.
577 Consequently, negative thermo-oxidative aging duration were calculated. Hence, new
578 aging-prediction models (i.e. identified as global aging-prediction models) were created,

579 including the factor of 'number of extrusion cycles'. Generally, these models exhibited a
580 good collinearity for the 'aging temperature' factor and the 'number of extrusion cycles'
581 factor. However, the 'aging time' factor of PET, PP and PE provided a collinearity lower
582 than 0.70. The models' estimation accuracy was also evaluated by calculating the
583 RMSE for each of the mentioned factors. The aging time factor was far from zero for all
584 tested polymers, yet the lowest value was obtained for ABS (47.48) and the highest for
585 PP (125.56). This was replicated when plastic waste samples were tested; the aging
586 time estimation was mostly negative in value, especially for ABS material. The
587 estimations of 'aging temperature and the 'number of extrusion cycles' were always
588 positive in values, where the most reasonable aging factor estimation was the 'number
589 of extrusion cycles'. All in all, the generated models need to be extended to include a
590 wider range of data, where further aging parameters, e.g. UV radiation (Picuno et al.
591 2019a) should be considered for the aim of including all possible forms and degrees of
592 degradation.

593 **Acknowledgements**

594 This research did not receive any specific grant from funding agencies in the public,
595 commercial, or not-for-profit sectors. The authors declare no interest in the research.
596 The authors gratefully acknowledge the contribution of Iryna Atamaniuk, Lucas Pfennig,
597 Arianna Prette and Giada Fenocchio in supporting the experimental activities of the
598 research.

599 **References**

600

601 Alassali, A.; Moon, H.; Picuno, C.; Meyer, R. S.A.; Kuchta, K. (2018a): Assessment of
602 polyethylene degradation after aging through anaerobic digestion and composting. In
603 *Polymer Degradation and Stability* 158, pp. 14–25.

604 Alassali, Ayah; Fiore, Silvia; Kuchta, Kerstin (2018b): Assessment of plastic waste
605 materials degradation through near infrared spectroscopy. In *Waste management* 82,
606 pp. 71–81. DOI: 10.1016/j.wasman.2018.10.010.

607 Al-Salem, S. M.; Lettieri, P.; Baeyens, J. (2009): Recycling and recovery routes of plastic
608 solid waste (PSW). A review. In *Waste management* 29 (10), pp. 2625–2643.

609 Anne Shayene Campos de Bomfim; Maísa Milanez Ávila Dias Maciel; Herman Jacobus
610 Cornelis Voorwald; Kelly Cristina Coelho de Carvalho Benini; Daniel Magalhães de
611 Oliveira; Maria Odila Hilário Cioffi (2019): Effect of different degradation types on
612 properties of plastic waste obtained from espresso coffee capsules. In *Waste*
613 *management* 83, pp. 123–130. DOI: 10.1016/j.wasman.2018.11.006.

614 Azadi, Sama; Karimi-Jashni, Ayoub (2016): Verifying the performance of artificial neural
615 network and multiple linear regression in predicting the mean seasonal municipal
616 solid waste generation rate: A case study of Fars province, Iran. In *Waste*
617 *management* 48, pp. 14–23.

618 Beninia, KCCC; Voorwald, Herman Jacobus Cornelis; Cioffi, M. O.H. (2011): Mechanical
619 properties of HIPS/sugarcane bagasse fiber composites after accelerated
620 weathering. In *Procedia Engineering* 10, pp. 3246–3251.

621 Bishop, Christopher M. (2006): Pattern recognition and machine learning: springer.

622 Blanco, M.; Villarroya, INIR (2002): NIR spectroscopy: a rapid-response analytical tool.
623 In *TrAC Trends in Analytical Chemistry* 21 (4), pp. 240–250.

624 Boldizar, Antal; Möller, Kenneth (2003): Degradation of ABS during repeated processing
625 and accelerated ageing. In *Polymer Degradation and Stability* 81 (2), pp. 359–366.

626 Brandrup, J. (1996): Recycling and recovery of plastics. Munich, New York: Hanser.

627 Broad, Neville; Graham, Paul; Hailey, Perry; Hardy, Allison; Holland, Steve; Hughes,
628 Stephen et al. (2002): Guidelines for the development and validation of near-infrared
629 spectroscopic methods in the pharmaceutical industry. In *Handbook of vibrational*
630 *spectroscopy* 5, pp. 3590–3610.

631 Chai, Tianfeng; Draxler, Roland R. (2014): Root mean square error (RMSE) or mean
632 absolute error (MAE)?—Arguments against avoiding RMSE in the literature. In
633 *Geoscientific model development* 7 (3), pp. 1247–1250.

634 da Costa, Helson M.; Ramos, Valéria D.; Oliveira, Márcia G. de (2007): Degradation of
635 polypropylene (PP) during multiple extrusions: Thermal analysis, mechanical
636 properties and analysis of variance. In *Polymer Testing* 26 (5), pp. 676–684. DOI:
637 10.1016/j.polymertesting.2007.04.003.

638 Denise Reike; Walter J.V. Vermeulen; Sjors Witjes (2018): The circular economy: New
639 or Refurbished as CE 3.0? — Exploring Controversies in the Conceptualization of the
640 Circular Economy through a Focus on History and Resource Value Retention
641 Options. In *Resources, Conservation and Recycling* 135, pp. 246–264. DOI:
642 10.1016/j.resconrec.2017.08.027.

643 Dopico-García, M. S.; Castro-López, M. M.; López-Vilariño, J. M.; González-Rodríguez,
644 M. V.; Valentao, P.; Andrade, P. B. et al. (2011): Natural extracts as potential source
645 of antioxidants to stabilize polyolefins. In *Journal of Applied Polymer Science* 119 (6),

646 pp. 3553–3559.

647 Faraca, Giorgia; Martinez-Sanchez, Veronica; Astrup, Thomas F. (2019): Environmental
648 life cycle cost assessment: Recycling of hard plastic waste collected at Danish
649 recycling centres. In *Resources, Conservation and Recycling* 143, pp. 299–309.

650 Goodfellow, Ian; Bengio, Yoshua; Courville, Aaron (2016): Deep learning: MIT press.

651 Hahladakis, John N.; Iacovidou, Eleni (2019): An overview of the challenges and trade-
652 offs in closing the loop of post-consumer plastic waste (PCPW): Focus on recycling.
653 In *Journal of Hazardous Materials* 380, p. 120887.

654 Hastie, Trevor; Tibshirani, Robert; Friedman, Jerome (2009): The elements of statistical
655 learning: data mining, inference, and prediction, Springer Series in Statistics:
656 Springer New York.

657 Holland, B. J.; Hay, J. N. (2002): The thermal degradation of PET and analogous
658 polyesters measured by thermal analysis–Fourier transform infrared spectroscopy. In
659 *Polymer* 43 (6), pp. 1835–1847.

660 Hopewell, Jefferson; Dvorak, Robert; Kosior, Edward (2009): Plastics recycling:
661 challenges and opportunities. In *Philosophical Transactions of the Royal Society of*
662 *London B: Biological Sciences* 364 (1526), pp. 2115–2126.

663 Horodytska, O.; Valdés, F. J.; Fullana, A. (2018): Plastic flexible films waste
664 management – A state of art review. In *Waste management*. DOI:
665 10.1016/j.wasman.2018.04.023.

666 Huth-Fehre, Th; Feldhoff, R.; Kantimm, Th; Quick, L.; Winter, F.; Cammann, K. et al.
667 (1995): NIR-Remote sensing and artificial neural networks for rapid identification of
668 post consumer plastics. In *Journal of Molecular Structure* 348, pp. 143–146.

669 Huysveld, Sophie; Hubo, Sara; Ragaert, Kim; Dewulf, Jo (2019): Advancing circular

670 economy benefit indicators and application on open-loop recycling of mixed and
671 contaminated plastic waste fractions. In *Journal of cleaner production* 211, pp. 1–13.

672 Izdebska, Joanna (2016): Aging and Degradation of Printed Materials. In Joanna
673 Izdebska, Sabu Thomas (Eds.): *Printing on Polymers*: William Andrew Publishing,
674 pp. 353–370. Available online at
675 <http://www.sciencedirect.com/science/article/pii/B9780323374682000221>.

676 Khoo, Hsien H. (2019): LCA of plastic waste recovery into recycled materials, energy
677 and fuels in Singapore. In *Resources, Conservation and Recycling* 145, pp. 67–77.

678 Krapf, Lutz Christian (2013): Evaluation of near infrared spectroscopy to estimate
679 process parameters in anaerobic digestion of agricultural feedstocks. Technische
680 Universität München.

681 M.K. Eriksen; K. Pivnenko; M.E. Olsson; T.F. Astrup (2018): Contamination in plastic
682 recycling: Influence of metals on the quality of reprocessed plastic. In *Waste*
683 *management* 79, pp. 595–606. DOI: 10.1016/j.wasman.2018.08.007.

684 Mandal, Himadri S.; Knaack, Gretchen L.; Charkhkar, Hamid; McHail, Daniel G.; Kastee,
685 Jemika S.; Dumas, Theodore C. et al. (2014): Improving the performance of poly (3,
686 4-ethylenedioxythiophene) for brain–machine interface applications. In *Acta*
687 *biomaterialia* 10 (6), pp. 2446–2454.

688 Masoumi, Hamed; Safavi, Seyed Mohsen; Khani, Zahra (2012): Identification and
689 classification of plastic resins using near infrared reflectance. In *International Journal*
690 *of Mechanical and Industrial Engineering* 6, pp. 213–220.

691 Murray, Kieran A.; Kennedy, James E.; McEvoy, Brian; Vrain, Olivier; Ryan, Damien;
692 Cowman, Richard; Higginbotham, Clement L. (2013): The effects of high energy
693 electron beam irradiation in air on accelerated aging and on the structure property

694 relationships of low density polyethylene. In *Nuclear Instruments and Methods in*
695 *Physics Research Section B: Beam Interactions with Materials and Atoms* 297,
696 pp. 64–74.

697 Ögütcü, Mustafa; Aydeniz, Buket; Büyükcan, Mehmet Burak; Yılmaz, Emin (2012):
698 Determining frying oil degradation by near infrared spectroscopy using chemometric
699 techniques. In *Journal of the American Oil Chemists' Society* 89 (10), pp. 1823–1830.

700 Pasquini, Celio (2003): Near infrared spectroscopy: fundamentals, practical aspects and
701 analytical applications. In *Journal of the Brazilian chemical society* 14 (2), pp. 198–
702 219.

703 Perugini, Floriana; Mastellone, Maria Laura; Arena, Umberto (2005): A life cycle
704 assessment of mechanical and feedstock recycling options for management of
705 plastic packaging wastes. In *Environ. Prog.* 24 (2), pp. 137–154. DOI:
706 10.1002/ep.10078.

707 Picuno, Caterina; Alassali, Ayah; Sundermann, Michel; Godosi, Zoe; Picuno, Pietro;
708 Kuchta, Kerstin (2019a): Decontamination and recycling of agrochemical plastic
709 packaging waste. In *Journal of Hazardous Materials*, p. 120965.

710 Picuno, Caterina; Godosi, Zoe; Kuchta, Kerstin; Picuno, Pietro (2019b): Agrochemical
711 plastic packaging waste decontamination for recycling: Pilot tests in Italy. In *Journal*
712 *of Agricultural Engineering* 50 (2), pp. 99–104.

713 Pojić, Milica; Mastilović, Jasna; Majcen, Nineta (2012): The application of near infrared
714 spectroscopy in wheat quality control. In : *Infrared spectroscopy-Life and biomedical*
715 *sciences*: IntechOpen.

716 Prestwich, Steven; Rossi, Roberto; Armagan Tarim, S.; Hnich, Brahim (2014): Mean-
717 based error measures for intermittent demand forecasting. In *International Journal of*

718 *Production Research* 52 (22), pp. 6782–6791.

719 Ragaert, Kim; Delva, Laurens; van Geem, Kevin (2017): Mechanical and chemical
720 recycling of solid plastic waste. In *Waste management* 69, pp. 24–58.

721 S. Brunner; P. Fomin; Ch. Kargel (2015): Automated sorting of polymer flakes:
722 Fluorescence labeling and development of a measurement system prototype. In
723 *Waste management* 38, pp. 49–60. DOI: 10.1016/j.wasman.2014.12.006.

724 Sánchez, Arnau Carné; Collinson, Simon R. (2011): The selective recycling of mixed
725 plastic waste of polylactic acid and polyethylene terephthalate by control of process
726 conditions. In *European Polymer Journal* 47 (10), pp. 1970–1976.

727 Shimada, Junichi; Kabuki, Kimiaki (1968): The mechanism of oxidative degradation of
728 ABS resin. Part I. The mechanism of thermooxidative degradation. In *Journal of*
729 *Applied Polymer Science* 12 (4), pp. 655–669.

730 Song, Qilei; Cao, Shuai; Pritchard, Robyn H.; Ghalei, Behnam; Al-Muhtaseb, Shaheen
731 A.; Terentjev, Eugene M. et al. (2014): Controlled thermal oxidative crosslinking of
732 polymers of intrinsic microporosity towards tunable molecular sieve membranes. In
733 *Nature communications* 5, p. 4813.

734 Thomas S. Gates (Ed.) (1999): On the use of accelerated aging methods for screening
735 high temperature polymeric composite materials. 40TH Structures, Structural
736 Dynamics, and Materials Conference and Exhibit.

737 Tiganis, B. E.; Burn, L. S.; Davis, Paul; Hill, A. J. (2002a): Thermal degradation of
738 acrylonitrile–butadiene–styrene (ABS) blends. In *Polymer Degradation and Stability*
739 76 (3), pp. 425–434.

740 Tiganis, B.E; Burn, L.S; Davis, P.; Hill, A.J (2002b): Thermal degradation of acrylonitrile–
741 butadiene–styrene (ABS) blends. In *Polymer Degradation and Stability* 76 (3),

742 pp. 425–434. DOI: 10.1016/S0141-3910(02)00045-9.

743 Venkatachalam, S.; Nayak, Shilpa G.; Labde, Jayprakash V.; Gharal, Prashant R.; Rao,
744 Krishna; Kelkar, Anil K. (2012): Degradation and recyclability of poly (ethylene
745 terephthalate). In : Polyester: InTech India, pp. 75–98.

746 Wahab, D. A.; Hussain, A.; Scavino, E.; Mustafa, M. M.; Basri, H. (2006): Development
747 of a prototype automated sorting system for plastic recycling. In *American Journal of*
748 *Applied Sciences* 3 (7), pp. 1924–1928.

749 Yu, Jie; Sun, Lushi; Ma, Chuan; Qiao, Yu; Yao, Hong (2016): Thermal degradation of
750 PVC. A review. In *Waste management* 48, pp. 300–314.

Online Supplementary Files_revised

[Click here to download Online Supplementary Files: Supplementary materials_revised.docx](#)